COMPUTATIONAL AND SYSTEMS
**ONCOLOGY**
Open Access

WILEY

# Boolean dynamic modeling of cancer signaling networks: Prognosis, progression, and therapeutics

**Shubhank Sherekar** | **Ganesh A. Viswanathan** [ORCID]

Department of Chemical Engineering, Indian Institute of Technology Bombay, Powai, Mumbai, India

**Correspondence**
Ganesh A. Viswanathan, Department of Chemical Engineering, Indian Institute of Technology Bombay, Powai, Mumbai 400076, India.
Email: ganeshav@iitb.ac.in

## Abstract

Cancer is a multifactorial disease. Aberrant functioning of the underlying complex signaling network that orchestrates cellular response to external or internal cues governs incidence, progression, and recurrence of cancer. Detailed understanding of cancer's etiology can offer useful insights into arriving at novel therapeutic and disease management strategies. Such an understanding for most cancers is currently limited due to unavailability of a predictive large-scale, integrated signaling model accounting for all tumor orchestrating factors. We suggest that the potential of Boolean dynamic (BD) modeling approaches, though qualitative, can be harnessed for developing holistic models capturing multi-scale, multi-cellular signaling processes involved in cancer incidence and progression. We believe that constraining such an integrated BD model with variety of omics data at different scales from laboratory and clinical settings could offer deeper insights into causal mechanisms governing the disease leading to better prognosis. We review the recent literature employing different BD modeling strategies to model variety of cancer signaling programs leading to identification of cancer-specific prognostic markers such as SMAD proteins, which may also serve as early predictors of tumor cells hijacking the epithelial-mesenchymal plasticity program. *In silico* simulations of BD models of different cancer signaling networks combined with attractor landscape analysis and validated with experimental data predicted the nature of short- and long-term response of standard targeted therapeutic agents such as Nutlin-3, a small molecule inhibitor for p53-MDM2 interaction. BD simulations also offered a mechanistic view of emerging resistance to drugs such as Trastuzumab for HER+ breast cancer, analysis of which suggested new combination therapies to circumvent them. We believe future improvements in BD modeling techniques, and tools can lead to development of a comprehensive platform that can drive holistic approaches

toward better decision-making in the clinical settings, and thereby help identify novel therapeutic strategies for improved cancer treatment at personalised levels.

## 1 | INTRODUCTION

Cancer is a multifactorial disease [1–3]. Cancer can be viewed as a result of disturbances of a delicate balance between cellular states, specifically proliferation and cell-death [4]. Identifying these disturbances and understanding their deleterious effects can help in better cancer prognosis, arresting tumor progression and improving the therapeutics needed for combating the disease. Systems biology-based Boolean dynamic (BD) modeling is an emerging approach for unraveling these disturbances which is paramount to developing strategies for restoring the delicate balance.

Worldwide, cancer incidence is 19.3 million per year, and cancer deaths stands at ∼9.9 million in 2020 [5]. Cancer incidence is expected to increase by ∼55% to 30.2 million per year by 2040 [6,7]. Current cancer care costs US\$ ∼1.16 trillion per year [8]. Large incidence rates coupled with rising associated costs makes the disease a public health priority and calls for arriving at effective strategies for preventing, managing, and combating it [7].

Cellular states are dynamically orchestrated by the underlying molecular network that responds to various external and internal stimuli [9]. Disturbances leading to dysregulation of a normal cellular state could be attributed to mutations affecting wiring of the network [2,9,10]. These mutations could be in proto-oncogenes and tumor supressing genes present in normal healthy cells. Influence of these disturbances could be far reaching, such as triggering metabolic reprogramming [10–15], evading apoptosis, a form of regulated cell-death [4,16–19]. These disturbances are caused by oncogenic or non-oncogenic factors which alter the information flow through the network [20]. Oncogenic factors include overactive forms of certain proto-oncogenes whose gain-in-function mutation drives cancer initiation. Non-oncogenic factors refer to loss-of-function of tumor suppressor genes leading to cancer development [21]. Identifying sections of the molecular network that are dysfunctional, the normal processes that are disturbed and the extent of ensuing damage can offer novel insights to diagnose, combat, and prevent these diseases [22].

Therapies for treating cancer capitalize on the specific molecular aspects in cancer cells that delineate them from normal cells. Conventional therapies using first or second line of treatment take advantage of the genetic instability reflecting deficiencies in DNA repair in the cancer cells [23]. Alkylating agents such as chlorambucil, cisplatin are used as first line chemotherapeutic drugs for inducing DNA damage and thereby arresting cancer cell proliferation. A second line of treatment includes use of drugs such as methotrexate or of ionizing radiation. Traditional cytotoxic drugs and radiation therapy are typically weakly selective [21,23]. As a direct consequence, these therapies may affect other normal cells and thereby causing severe undesired side-effects [24–26]. This led to the advent of targeted therapy which involves use of drugs targeting a cancer-specific malfunction such as those caused by a mutation. Targeted therapies for various cancers offer improved remission and overall survival as compared to the conventional approaches [24–26]. However, they are often hampered by natural or acquired resistance to drugs. Knowledge of the mechanisms governing a cancer can offer insights toward addressing this challenge. While identification of precise causal mechanisms governing a particular cancer is often difficult, even partial knowledge of these can help finding effective therapy that may circumvent emergence of drug resistance [27]. A systematic assessment of a system-level model of oncological signaling which orchestrates cell fate can help discern such causal mechanisms. Further, such a model can serve as an *in silico* platform for rigorously testing system-level effects of a certain drug and also provide pointers for novel therapeutic approaches and other clinical decisions [28].

Systems biology driven cancer models permit integration of oncological signaling in a tumor cell and its microenvironment, and regulation at protein-protein and genetic levels. Among various systems-level modeling approaches [29], logical models, such as those based on Boolean networks, enable unraveling qualitative principles that elucidate mechanisms governing various behaviors elicited by cells [30–34] and particularly that of oncological outcomes [35]. Since its first use [36], BD models are routinely used in characterizing several naturally observed attributes of biological systems such as underlying complexity [37–39], self-organizing

principles [40], redundancy, [41] and other nonlinear aspects [42,43]. BD approach offers a significant promise for understanding cancer's etiology from a signaling dynamics perspective and help identifying novel targeted therapies [35,44].

The present review is concerned primarily with BD modeling of cancer signaling networks with an emphasis on identifying principles governing various cancer-related processes. In the next section, we present a primer on BD modeling, which can be skipped by readers who are either familiar with it or are primarily interested in the BD modeling-based predictions. In the subsequent three sections, we review various BD modeling-based contributions leading to identification of diagnostic markers, deciphering mechanisms governing cancer progression, and understanding drug responses elicited by tumors.

## 2 | BD MODELING OF BIOLOGICAL NETWORKS

Building a BD model of a normal or diseased cell necessitates availability of an underlying molecular network governing the signal transduction process. A biological network consists of entities such as proteins, genes, small molecules, and the causal relationships as interactions between them. In this section, we first present a general formalism for BD modeling. Subsequently, we describe systematic approaches for constructing cancer-specific annotated signaling network.

### 2.1 | A primer on BD modeling

In this primer, we describe the BD modeling approach, its implementation and associated strategies using a cancer progression signaling network as a motivating example. These are applicable to signaling networks such as protein-protein networks (PPNs) [45], gene-transcriptional networks (GTNs) [46], multi-cellular networks, [47,48] and a combination thereof [49,50]. PPNs consisting only of interacting proteins are typically employed in cancer modeling when the objective is to understand how signal flow from a receptor is disturbed due to a malfunctioning entity in the network. Moreover, it is considered for identifying potential diagnostic and therapeutic protein markers. On the other hand, GTNs typically consist of transcription factors as entities. An interaction in a GTN represents regulation of its synthesis via the transcription and translation machinery by other transcription factors. GTNs are considered in cancer modeling for a variety of purposes such as understanding reprogramming triggered by oncogenic genetic abnormalities [51,52]. Multi-
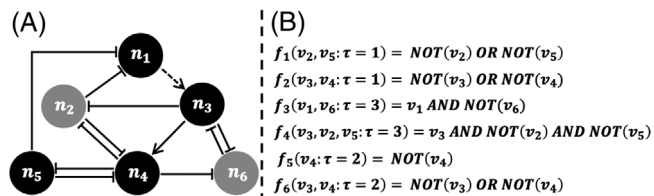


**FIGURE 1** Boolean dynamic modeling. (A) Six-node network based on TGF$\beta$ signaling in cancer cells.[53] Nodes $n_1$, $n_2$, $n_3$, $n_4$, $n_5$, and $n_6$ represent TGF$\beta$, miRNA200, Snail1, Zeb1, Ovol2, and miRNA34a, respectively. Black and grey circles, respectively, are proteins and microRNAs. Dashed arrow ($-\rightarrow$) captures activation of $n_3$ by node $n_1$. While solid arrows ($\rightarrow$) represent transcriptional activation, hammers (⊣) represent transcriptional inhibition. (B) Boolean functions $f_1$, $f_2$, ..., $f_6$ corresponding to the six nodes in (A). $\tau$ captures the timescale of activation of the node, applicable only for the case of deterministic asynchronous update method. $v_1, v_2, ..., v_6$ represent the Boolean values corresponding to the six nodes in (A)

cellular networks consist of multiple cells themselves as nodes or as compartments with sub-networks in each of them.

For demonstrating BD modeling of biological networks, we consider a six-node network consisting of signed, directed interactions based on TGF$\beta$ signaling in a cancer cell [53] as a motivating example (Figure 1A). TGF$\beta$ signaling is implicated in cancer progression [54]. TGF$\beta$, a secreted cytokine protein, upon binding to its receptor triggers signaling via MAPK cascade that culminates in activating the synthesis of Snail1 protein. Snail1 transcription factor activates Zeb1 and represses miRNA200. Moreover, Snail1 represses the transcription of miRNA34a and in turn miRNA34a inhibits Snail1 protein by modulating its translation. Thus, Snail1 and miRNA34a are locked in a double negative feedback loop. A similar double negative feedback loop exists between Zeb1 and miRNA200. On the other hand, Ovol2 and Zeb1 interlock each other via a transcriptional double negative feedback loop. Further, Zeb1 and Ovol2 transcription factors repress miRNA34a and the synthesis of TGF$\beta$, respectively. For the sake of brevity, we represent TGF$\beta$, miRNA200, Snail1, Zeb1, Ovol2, and miRNA34a, respectively as $n_1, n_2, ..., n_6$.

*BD network model* : A node ($n_i$) in the network is assumed a Boolean variable taking a logical value FALSE or TRUE captured by $\{v_i = 0\ or\ 1\}$, respectively, representing inactive, that is, not-expressed (OFF) or active, that is, expressed (ON) forms of the entity. In case of proteins, expressed and not-expressed reflect high and low concentrations, respectively. Node $n_i$ is associated with a Boolean function $f_i$ consisting of logical operations AND, OR, or NOT governed $m$-logical-rules corresponding to $m$ binary inputs to it. $f_i$ determines the

**TABLE 1** States reached in the first few timesteps starting from initial state ( $s_0 = 101001$) using synchronous (S), deterministic asynchronous (DA), general asynchronous (GA), and random order asynchronous (ROA) update schemes. Nodes updated at a time $t$ using the Boolean functions in Figure 1B are in red with the value of all others retained as is. While FP reached for S, and DA methods are specified by the state at t $= \infty$, that for GA and ROA methods depend respectively on randomly chosen update order and the randomly chosen permutations at every $t$. For the case of DA, timescale $\tau$ is specified in Figure 1B. Permutations used for ROA for $t = 1, 2, 3$, respectively, are 431562, 564132, and 164325

| Nodes | S | | | | DA | | | | GA | | | ROA | | |
|---|---|---|---|---|---|---|---|---|---|---|---|---|---|---|
| t → | 1 | 2 | 3 | ∞ | 1 | 2 | 3 | ∞ | 1 | 2 | 3 | 1 | 2 | 3 |
| $n_1$ | 1 | 0 | 1 | 0 | 1 | 1 | 1 | 0 | 1 | 1 | 1 | 1 | 1 | 1 |
| $n_2$ | 1 | 1 | 1 | 1 | 1 | 1 | 1 | 1 | 1 | 1 | 1 | 1 | 1 | 1 |
| $n_3$ | 0 | 0 | 0 | 0 | 1 | 1 | 0 | 0 | 1 | 1 | 1 | 0 | 0 | 0 |
| $n_4$ | 1 | 0 | 0 | 0 | 0 | 0 | 0 | 0 | 0 | 0 | 0 | 1 | 0 | 0 |
| $n_5$ | 1 | 0 | 1 | 1 | 0 | 1 | 1 | 1 | 0 | 0 | 1 | 0 | 0 | 1 |
| $n_6$ | 1 | 1 | 1 | 1 | 1 | 1 | 1 | 1 | 1 | 1 | 1 | 1 | 1 | 1 |

value taken by $n_i$ due to the logical operations resulting from $m$ inputs. Thus, the BD of the six-node network can be captured by the dynamics of the variables $\{v_i = 0 \text{ or } 1, \forall i\}$ governed by the functions $\{f_i, \forall i\}$ (Figure 1B). For example, $n_2$ and $n_5$ inhibit $n_1$ resulting in $f_1(v_2, v_5) = NOT(v_2) OR NOT(v_5)$, where an OR logic is assumed for the two inhibitory inputs (Figure 1). The dynamics to the Boolean model is introduced by updating $v_i$ using $f_i$ evaluated at the prior values of those nodes contributing to the logical-rules in it [36]. The value taken by $v_i$ depends on the update scheme adopted, which we discuss next.

A synchronous (S) update scheme is one where $v_i \forall i$ is updated simultaneously, that is, at time $t + 1$, $v_i^{t+1} = f_i(v_1^t, v_2^t, .., v_6^t)$ [46,55–57]. Starting from a random initial state $s_0 = \{v_1^0, v_2^0, v_3^0, v_4^0, v_5^0, v_6^0\} = \{1, 0, 1, 0, 0, 1\}$, one S update results in network's state ($s_1$) being 110111, with each digit representing the Boolean value (Table 1) taken by the corresponding node [43,58]. For the sake of brevity, henceforth, a network's state will be presented as six binary digits randomly assigned to six nodes in Figure 1A. Upon repeated updating, after visiting several transient states, the network reaches a Boolean steady state of 010011 (Table 1). Such a steady state is referred to as an absorbing-state or fixed-point (FP) attractor or FP. Set of initial states culminating in FP forms its basin of attractor. Note that value taken by nodes at FP indicates the active or inactive entities in the cell under homeostasis and thereby reflecting its phenotype. Besides FPs, a network can also reach cyclic attractors, in which transients hover around periodic sequence of states [59]. S update method is known to lead to several spurious cyclic attractors [59].

In biological systems, all nodes are not necessarily activated simultaneously. Asynchronous update scheme via deterministic asynchronous (DA), general asynchronous (GA) and random-order asynchronous (ROA) methods

permits staggered updating of nodes [43,60]. Nodes to be updated are either randomly chosen or specified by a priori known discrete activation timescale $\tau$ for every entity [43,60]. For DA method, at every $t$, only nodes with $\tau \leq t$ are updated [48]. Table 1 shows $s_1, s_2, s_3$, and $s_\infty$(FP) obtained by starting from $s_0$. FP reached from an initial state is identical and unique for both S and DA methods. On the other hand, GA and ROA methods are applicable when $\tau$ is unavailable and further, permit capturing stochasticity, a phenomenon naturally present in biological systems [61,62]. In GA method, at every $t$, a randomly chosen node is updated leading to reaching an *update-order dependent* FP from an initial state [45]. Same $s_0$ leads to different dynamic states for S, DA, and GA methods (Table 1). In ROA method, at every $t$, 1. updating is further resolved into as many intervals as that of the number of nodes, and 2. all nodes are updated in a certain sequence (permutations), chosen uniformly randomly [50]. GA approach captures the stochasticity due to the cascading effect of updating randomly chosen individual nodes over several timesteps. On the other hand, ROA allows incorporating the stochastic behavior originating from the interdependency of the nodes at all timesteps. Table 1 shows states reached in three successive instances, each employing different permutations, with $s_0 = 101001$. All three update methods can lead to cyclic attractors. In fact, the spurious cyclic attractors predicted by the S method can be circumvented by using asynchronous update schemes [59]. However, GA and ROA can in addition lead to complex attractors wherein the transients meander over a set of states in no specific order.

An extension of a BD model is the multivalued discrete dynamic network model wherein $v_i$ can take multiple integers [31]. This allows capturing varying levels of each of the nodes. Further, every rule in the function governing the dynamics of a node is scaled with a weight factor that
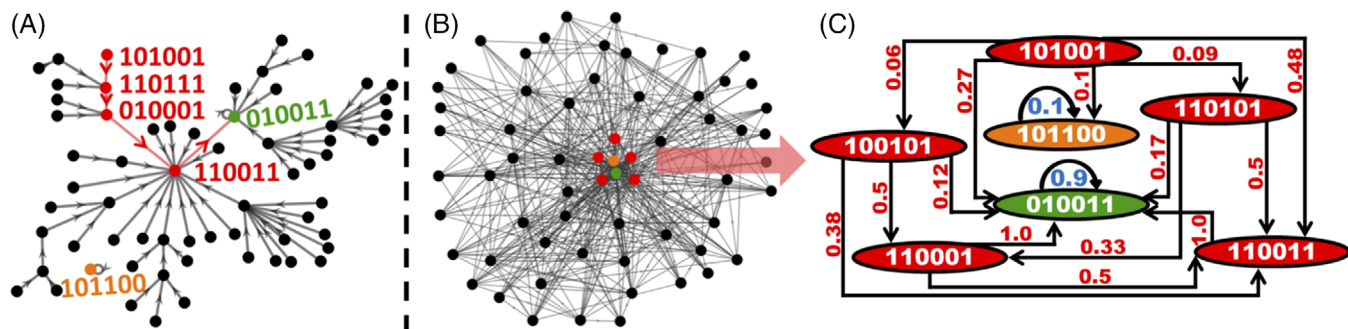
**FIGURE 2** (A) Complete state transition graph (STG) showing states (dots) and one-step transitions (arrows) between them obtained using synchronous update method. Self-arrow to a state indicates FP. Red dots show the transients obtained to reach the FP 010011 (green) with initial state $s_0$ being 101001. Orange dot represents FP 101100. (B) Complete STG obtained using ROA update method. (C) Partial STG, a section of the complete STG in (B), consisting of seven states (dots highlighted in [B]) and all one-step transitions between them. Initial state is $s_0$ = 101001. Probability of reaching FPs from $s_0$ is shown within the self-arrow. Numbers (in red) placed next to the one-step transition arrow captures the associated transition probability calculated by incorporating the corresponding number of permutations in Table 2 into Equation (1)

captures the multivalued nature of $v_i$. Simulations of the discrete dynamics of the model using the multivalued $v_i$ and the modified functions are performed using synchronous and asynchronous update schemes described above. Besides the ensuing computational complexities, deciding the range for the multivalued variables is often a challenge. A comprehensive list of toolboxes for performing discrete dynamic model simulations is available at The CoLoMoTo consortium [63].

*Long-term behaviour of a BD model* : Analyzing the transients, due to one-step transitions, reached while traversing from $s_0$ to desired FP can offer insights into network's inclination to reach a phenotype. A collection of such one-step transitions achieved by starting from all possible 64 ( $= 2^6$ ) initial states is the six-node network's state-transition-graph (STG) which has states as nodes connected by one-step transitions as directed interactions and can be constructed for all four update methods [59]. For the case of synchronous update, Figure 2A shows the complete STG. The states reached while traversing from $s_0 =$ 101001 to reach the FP 010011 are captured in Figure 2A (red dots). STG also shows that the FP 101100 (orange dot) can be reached via synchronous update only when the initial state is itself. Thus, all states other than FP 101100 belong to the basin of attraction of FP 010011. Note that the path taken to reach an FP from an initial state is unique when S update method is employed, as corroborated by the STG for the six-node network (Figure 2A). On the contrary, the path traversed to reach an FP starting from an initial state is non-unique for the case of GA and ROA methods. Thus, stochasticity incorporated in GA and ROA methods permits expansion of the basin of attractors for reaching different FPs, a feature exhibited by real networks [45]. In Figure 2B, we show the complete STG

for the six-node network when ROA method is employed. STG captures the permutation-dependent path to reach an attractor from any state that the network can take. For example, starting from $s_0 =$ 101001, one-step transitions caused by permutations 451236 and 416325 lead to states 100101 and FP 101100, respectively. Thus, depending upon the path dictated by the permutations chosen for the intermediate timesteps, ROA method takes $s_0 =$ 101001 to either 010011 or 101100 FP, as shown in the partial STG in Figure 2C. Thus, multiple paths could lead to same FP. Note that multiple permutations could cause same one-step transition. For ROA method, since every one-step transition will have an underlying permutation, STG will have utmost 46, 080 ( $=$ 64 × 6! $=$ 64 × 720) transitions. For a large network, finding complete STG is computationally tedious. However, experience suggests that a much smaller STG could aptly capture the required characteristics, particularly that of the driver entities that govern the network's dynamics and of the attractors.

Ability of a network to settle into an FP is quantified by the probability which can be estimated from the STG. This probability can help unravel network's features such as driver entities. The first step in this quantification process is finding the 1-step state transition matrix $T$. An element $T_{ij}$ of this matrix specifies the probability of achieving a one-step transition from $s_i$ to $s_j$ and is given by [59,64]

$$T_{ij} = \frac{z_{ij}}{\sum_{all\ j} z_{ij}} \tag{1}$$

where, $z_{ij}$ is the number of permutations causing the transition. Number of permutations causing the one-step transitions in the partial STG is in Table 2, and the

**TABLE 2** Number of permutations causing the one-step transitions in the partial STG in Figure 2C obtained using ROA update method. FPs are shown in boldface

| Start state ($s_i$) | End state ($s_j$) | Number of permutations ($z_{ij}$) | Start state ($s_i$) | End state ($s_j$) | Number of permutations ($z_{ij}$) |
|---|---|---|---|---|---|
| 101001 | 100101 | 42 | 110011 | **010011** | 720 |
| 101001 | **101100** | 72 | 110101 | 110001 | 360 |
| 101001 | 110101 | 66 | 110101 | 110011 | 240 |
| 101001 | 110011 | 348 | 110101 | **010011** | 120 |
| 101001 | **010011** | 192 | 110001 | **010011** | 360 |
| 100101 | 110001 | 360 | 110001 | 110011 | 360 |
| 100101 | 110011 | 270 | **010011** | **010011** | 720 |
| 100101 | **010011** | 90 | **101100** | **101100** | 720 |

corresponding transition probabilities estimated using Equation (1) are presented in Figure 2C. An iterative solution of

$$p = T \cdot p \qquad (2)$$

starting from the initial vector $p_0 \equiv$ $\begin{cases} p_{0k} = 1, \& \ s_k = s_o \\ p_{0k} = 0, \& s_k \neq s_0 \end{cases}$ gives the probability of reaching different FPs starting from $s_0$. Setting the initial vector $p_0 \equiv \{ p_{0k} = 1/l, \forall k \}$, where $l$ is the number of states in the STG, gives the average or steady-state probability of absorbing into different FPs of the STG. Steady-state probabilities of reaching the two attractors 010011 and 101100 estimated using Equation (2) are 0.9 and 0.1, respectively (Figure 2C).

## 2.2 | Biological network construction

Often network of interest may be unavailable. As a result, constructing a reliable, domain-specific signaling wiring diagram of a normal healthy cell is the logical starting point for building a BD model. Note that domain-specific refers to specific tissue of interest and the type of the wiring diagram considered. The first step toward constructing a network is curation of information about the nodes and interactions between them. A comprehensive review of nature of different entities and interactions is in Papin et al. [65]. Two broad approaches for biological network curation and construction are data-driven objective and knowledge-driven objective [66,67]. Data-driven objective employs available experimental data, for example, in-house generated microarray/proteomics data, those in GEO repository [68], ExpressionAtlas [69], GeNet [70,71]. On the other hand, knowledge-driven objective involves mining information from pre-curated databases such as STRING [72], InWeb [73], OmniPath [67], Reactome [74], Ingenuity [75], relevant primary experimental literature, either manually or using automated software tools. DREAM challenge data [76], genetic dependencies repositories [77–81], and cancer-specific mutated genes database CCLE [82] provide cancer-specific information. Entities and interactions thus distilled can be visualized as a wiring diagram using software such as CellDesigner [83], Cytoscape [84], which stores it in a portable, shareable, machine-readable format [85]. Collected information is further structured and refined to include cancer-type-specific annotations such as tissue, nature of activation, associated logic. Annotations form the basis for arriving at a logical function governing activation of a node in BD modeling framework, detailed in section 2.1. After construction, a series of network reduction by identifying key structures [86] or removing certain variables such as frozen nodes [39,43,87–89] curtails computations. Systematic step-wise network construction methodology and compendium of resources are available in Türei et al. [67]

## 3 | MARKERS GOVERNING PHENOTYPE SWITCHING

Early diagnosis of tumor formation is extremely useful in employing effective treatment regimens [90]. Cancer being a multifactorial dynamic signaling problem involving multitude of interacting entities, aberrant nodes serves as markers for (early) diagnosis, thereby facilitating better disease management. For cancers exhibiting strong variability in clinical response to therapies, markers distinguishing disease severity and reflecting therapeutic outcome help stratifying patients for an appropriate treatment [90–93]. In this section, we review BD approaches to model switching of inflammation or apoptosis to proliferation phenotype and thereby identify diagnostic markers. Networks considered in this section span from only-apoptosis

**TABLE 3** Cancer diagnostic markers predicted by Boolean dynamic modeling of various networks. Construction objective adopted and the network statistics are specified. S and GA refer respectively to synchronous and general asynchronous update methods described in section 2.1

| Cancer type | Construction objective | Compartment | Nodes | Links | Update scheme | Diagnostic markers |
|---|---|---|---|---|---|---|
| Inflammation to proliferation phenotype switching | | | | | | |
| Colon cancer [49] | Knowledge-driven | Intracellular and tumor microenvironment | 70 | 153 | GA | Sustained DC and p53 inactivation |
| Pan-cancer [97] | Knowledge-driven | Intracellular | 40 | 58 | S | p53 inactivation |
| Evading apoptosis attractor | | | | | | |
| Pan-cancer [102] | Knowledge-driven | Intracellular | 25 | 45 | S and GA | APAF1, Bax, FADD in presence of TNF$\alpha$ |
| Neurodegenerative Diseases [103] | Knowledge-driven | Intracellular | 21 | 37 | S | Overexpression of HSP70 |
| Pan-cancer [104] | Knowledge-driven | Intracellular | 96 | 249 | GA | APC and SMAD4 deletion |
| Breast cancer [106] | Knowledge-driven | Intracellular | 13 | 21 | GA | Malfunctioning of PTEN and Gsk3$\beta$ |
| Leukemia [45] | Knowledge-driven | Intracellular | 60 | 142 | GA | SMAD, PLCG1 |
| Pan-cancer [107] | Knowledge-driven | Intracellular | 23 | 37 | GA | Dysfunctioning of SMAD2 and SMAD3 |
| Bladder carcinomas [109] | Knowledge-driven | Intracellular | 53 | 112 | GA | MAPK pathway effective in FGFR3 not in EGFR |

to pan-cancer to a specific cancer-tissue. These networks could consist of entities within a cell or additionally those accounting for multicellular signaling events in the tumor microenvironment. For every case considered, network details, the Boolean modeling update scheme adopted and key findings are presented in Table 3. Malfunctioning and overexpression of an entity due to a certain mutation is captured by node deletion or node over-expression (ON), respectively.

## 3.1 | Inflammation to proliferation phenotype switching

Cancer cells secrete inflammatory cytokines and chemokines and thereby induce inflammation in the neighbouring cells [2,94]. Inflammatory cells in turn promote cancer progression by making them to commit to proliferation phenotype [95,96]. This phenotype switching is an important step in cancer progression. Entities involved in this switching process can thus serve as diagnostic markers [96].

Analysis of FP, cyclic, and complex attractors of a colitis-associated colon cancer network showed that transient dendritic cell activation, an essential step for a successful immune response, is needed for a release of inflammatory

cytokines and chemokines [49]. Entities considered in the network include immune cells in tumor microenvironment such as dendritic cells, secreted cytokines and chemokines, and intracellular signaling nodes. This analysis further showed that simultaneous sustained dendritic cell activation and p53 protein inactivation may govern the inflammatory to proliferation phenotype switching [49]. BD attractor analysis of an (pan-cancer) apoptosis network corroborated that inactivation of p53 results in breaking key feedback loops which serve as an alternative for irreversible apoptotic cell fate when those with normal caspase-3 are dysfunctional [97].

Recently, a novel approach of finding the Hierarchical Partitioning for the Phenotype, implemented on the colitis-associated colon cancer network [49], offers promise in finding the global attractors corresponding to a specific phenotype [98]. This approach involved pre-evaluating the Boolean functions with the phenotype-specific value corresponding to the external nodes. This results in a simplified sub-network with interactions governed by fully- or semi-updated rules that uniquely specify the attractors corresponding to the phenotype. In order to identify the markers that may be controlling the proliferation phenotype, the model was analysed by assuming sustained activation of adenomatous polyposis coli protein representing premalignant epithelial cells and dendritic cells.

This analysis suggested that SOCS, JAK, and STAT3 may be controlling the proliferation global attractor. Moreover, the analysis also revealed that during sustained dendritic cell activation, the model does not predict apoptotic phenotype.

## 3.2 | Proliferation phenotype by evading apoptosis

One of the hallmarks of cancer is evading apoptotic signaling [2]. In normal cells, TNF superfamily cytokines TNF$\alpha$ and FASL [99] maintain a balance between the apoptotic, necrotic, and proliferative phenotypes [100]. Note that the precise role of TNF superfamily cytokines in driving different cell-types into these different phenotypes is still under investigation [101]. Under various pathological conditions, cells secrete large quantities of TNF$\alpha$ leading to an elevated leads of the cytokine in the tissue microenvironment. Steady-state probability of a TNF$\alpha$-FASL signaling network for reaching different phenotypes could delineate the roles played by various cancer-associated pro- and anti-apoptotic genes [102]. Even when TNF$\alpha$ is active, deletion of APAF1, BAX, FADD, or Caspase 8, or overexpression of BCL2 or NF$\kappa$B is sufficient to switch the steady-state probability significantly toward anti-apoptotic phenotypes [48,102]. FP attractor analysis of a BD model of neuronal cell network activated simultaneously with FASL and neuronal growth factor showed that overexpressed HSP70 shock protein dominates over HSP27, HSP40, and HSP90 in promoting proliferation of cells, which would otherwise commit to apoptosis [103]. Systematic experimentation on Neuro2a cell line substantiated this prediction. Further, the attractor analysis identified BCL2, IAP, cFLIP, and NF$\kappa$B as key players of pro-survival cell fate.

An integrated PPN of signaling pathways was analyzed systematically for assessing the nature of stability of attractors corresponding to apoptosis, proliferation, and quiescent phenotypes [104]. Analysis of FP and complex attractors of the network under 32 distinct environmental conditions predicts that 1. under normoxia conditions, deletion or overexpression of 10 proteins such as EGFR, NF$\kappa$B, Ras can transform quiescent cells into proliferative ones, and 2. under hypoxia conditions, the repertoire of deleted or overexpressed proteins promoting proliferation increases by 7 over and above those under normoxia conditions. Further, deletion of APC, p53, Smad4, pTEN and overexpression of RAS, Tcf, Akt in the network to mimic colorectal carcinoma [105] led to switching of 97% apoptosis/quiescence attractors under normal conditions to 50% taking proliferation phenotype. BD model of an EGFR+ breast cancer network predicted that proliferation

phenotype requires malfunctioning of PTEN or GSK3 $\beta$ [106]. Moreover, structural and topological analysis of the attractors of a T-cell large granular lymphocyte leukaemia network led to identification of entities such as RAS, PLCG1, IAP, SMAD as key for apoptosis to proliferation phenotype switching [45] with the role of SMAD substantiated experimentally.

MAPK pathways are known to be sentinels of cancer. TGF$\beta$ signaling exhibits dual role in cancer cells by context-specifically regulating apoptosis and proliferation phenotypes. While it acts as a tumor-supressor via p38-MAPK pathways in normal or early cancer cells by arresting cell-cycle or triggering apoptosis, its tumor-promoting role in the late-stages leading to cells choosing proliferation attractor is attributed to the dysfunction of SMAD2 and SMAD3 proteins [107]. Ability of signaling through activated MAPK pathways to facilitate a balance [108] between the proliferative and non-proliferative phenotypes makes the FGFR3-mutated bladder carcinomas less aggressive [109].

In summary, BD modeling approaches implemented on different cancer-tissue-specific networks led to identification of markers that drive inflammation to proliferation phenotype switching and lead to acquiring proliferation cell-fate by evading apoptosis. Tracking these markers can help early stratification of patients and thereby facilitating improved management of the disease.

## 4 | CANCER PROGRESSION: EPITHELIAL-MESENCHYMAL PLASTICITY

Cancer progression involves tumor growth, evolution, invasion, and spreading. In order to achieve these, cancer cells capitalize on the normal cell-biological program called epithelial-mesenchymal plasticity (EMP) [110,111]. EMP facilitates adaptation of cancer cells to a new environment [112]. Moreover, it may even induce drug resistance in them [113]. EMP consists of multiple possible phenotypic states with complete epithelial-to-mesenchymal transition (EMT) and complete mesenchymal-to-epithelial transition (MET) at the two ends of the spectrum [53,114–117]. A cancer cell hijacks the EMT process to leave the primary tumor site for invading surrounding tissues and thereafter, migrate, and enable distant metastasis [112,118]. Significant fraction of cancer-related mortality is associated with metastasis [119]. An outstanding question is, what are the factors that dictate distal-organ invading abilities of a cancer cell? Mechanistic insights into EMT can offer clues to arresting or controlling this cell-biological program hijacked by the cancer cell. An emerging strategy to unravel topological features and causal mechanisms

**TABLE 4** Cancer progression markers predicted by Boolean dynamic modeling of various networks. Construction objective adopted and the network statistics are specified. S, GA, and ROA refer respectively to synchronous, general asynchronous, and random-order asynchronous update methods described in section 2.1

| Cancer type | Construction objective | Compartment | Nodes | Links | Update scheme | Progression markers |
|---|---|---|---|---|---|---|
| | | Epithelial-mesenchymal plasticity | | | | |
| Bladder cancer [86] | Knowledge-driven | Intracellular | 41 | 107 | S | E2F1, TGFBR1, FGFR1 |
| Breast cancer [86] | Knowledge-driven | Intracellular | 35 | 86 | S | E2F1, TGFBR2, EGFR |
| Hepatocellular carcinoma [120] | Knowledge-driven | Intracellular | 70 | 135 | GA | SMAD with Wnt, SHH, AKT, or MAPK |
| Hepatocellular carcinoma [124] | Knowledge-driven | Intracellular | 65 | 136 | GA | SMAD with Ras, NOTCH or SOS/GRB2 |
| Pan cancer [125] | Knowledge-driven | Intracellular and tumor microenvironment | 30 | 156 | GA | Notch overexpression and p53 deletion |
| Smaller cell lung cancer [129] | Data-driven | Intracellular | 33 | 361 | ROA | INSM1, SOX2, Ovol2, FOXA2- NE; MYC, NFκB1, SMAD3- ML |

governing tumor invasion, EMT, and migration is to systematically analyze GTN constructed using large gene-expression data from different cancer patient cohorts. Table 4 contains the network details, the BD modeling update scheme adopted, and key findings for the cases reviewed in this section. BD model of bladder and breast cancer juxtaposed with independent experimental studies led to prediction of E2F1, TGFBR2, and EGFR being important molecular signatures for regulation of tumor invasion and thereby EMT [86].

TGF$\beta$ induces a trans-differentiation program enabling the epithelial phenotype characterized by adhesion properties such as tight junctions to create mesenchymal derivatives such as better mobility due to loss of E-cadherin and overexpression of vimentin [54]. This induction of EMT occurs in cooperation with the activation of SONIC Hedgehog and Wnt-SHH pathways [120]. Activation of Wnt signaling, implicated in EMT triggered by different cancer [121,122], may even induce drug-resistance [122,123]. A systematic combinatorial node perturbations on a BD model of EMT in Hepatocellular carcinoma complemented with siRNA-based experimentation showed that inhibition of SMAD along with RAS, NOTCH, or SOS/GRB2, which hamper the key feedback loops, is effective in suppressing TGF$\beta$-induced EMT [124]. However, inhibition of SMAD alone results in a hybrid EMT state where cells exhibit both epithelial and mesenchymal traits.

Local invasion by and eventual late-stage migration of cancer cells must have myriad signatures in the early stages of metastasis. In the case of gut cancer, simultaneous Notch overexpression and p53 deletion in a TGF$\beta$-induced EMT network drives settling of cells exhibiting invasion or EMT or other phenotypic attractors into a metastatic one [125]. This suggests that the synergistic effect could have favored migration, as has been corroborated by experiments in mouse gut [126].

Phenotypic variability expressed by small-cell lung cancer, which is aggressive in terms of its ability to relapse post-first line of treatment, constitutes presence of both neuroendocrine/epithelial (NE) and non-neuroendocrine/mesenchymal (ML) behaviours [127]. Attractor analysis of the underlying transcription network, constructed using expression data from clinical samples [82,128], revealed specific coexistence of NE and ML sub-populations. The coexistence of such epithelial and mesenchymal characteristics has been validated *in vitro* on several small-cell lung cancer cell lines [129]. Further, the Boolean value taken by the identified attractors suggested that while INSM1, POU3F2, SOX2, SOX11,FOXA2, OVOL2 genes may be responsible for the NE behavior, MYC, NFKB1, SMAD3 genes are active in the ML phenotype. *In vitro* single-cell study further revealed that after cells were treated with first line (cytotoxic) drugs, the two sub-populations transited into hybrid EMT phenotype [129].

Cells are constantly exposed to internal and external noise, sources for which are plenty [61,62]. Even though BD models predict the attractors corresponding to different cellular states, it is well-known that EMT may involve multiple intermediates [130–133]. Given the inherent stochastic environment cancer cells may experience, gaining confidence on the causal mechanism governing these different attractors requires stability analysis of these multiple states [134]. Relative stability of an attractor is quantified by

comparing effort required for the network to switch from one FP to another [112]. Recently, dynamic stability analysis of attractors of a generic GTN underlying EMT showed that attractor corresponding to the epithelial phenotype is more stable than the others [134]. The dynamic stability was estimated based on the one-degree neighborhood of cell states [134].

New emerging evidences suggest that blocking EMP in both directions, that is, EMT and MET, and holding the cancer cells in its current relative epithelial-mesenchymal state may help reduce its ability to adapt to fluctuating environments and thereby, decrease its metastatic potential [135]. Recently, a combined topological and BD analysis of the EMT network identified key positive feedback loops that may govern E/M phenotypic multistability, the extent of its influence, and the deletion of interactions controlling plasticity [136]. In order to account for heterogeneity, dynamic variability in the Boolean value taken by an entity was introduced by linking the decision for updating a node at a certain timestep to the relative number of instantaneous activating or inhibitory inputs at that instant [137].

In summary, various BD modeling approaches have been employed to model cancer progression via the EMT for different cancer types. Molecular signatures governing EMT were identified using systematic perturbation analysis. Dynamic stability analysis of the attractors revealed key underlying topological features modulating the phenotypic multistability involved in the EMT. These findings can be utilized to better control the cancer cell's ability to hijack the EMP.

# 5 | THERAPEUTIC OUTLOOK: DRUG RESPONSE AND RESISTANCE

The plethora of drugs is available for different cancers [138], several of which are in various stages of clinical trials [139]. Various first and second line of therapeutic agents – for example, Gefitinib for the non-small cell lung-cancer [140] approved for targeted therapies are typically based on the mutation that drives tumor formation and do offer some promise like improved remission compared to traditional chemotherapy [24,25,26,141]. However, the overall efficacies of these approaches are also fraught with varying susceptibility or side-effects or intrinsic resistance to drugs or induced drug-resistance, just as in the case of the conventional therapies. Thus, finding cancer-specific targeted therapies that circumvent these challenges continues to remain an open quest. BD modeling-based strategies for attractor switching, particularly to apoptosis, identified *in silico* are valuable in finding potential candidates for design of better interventional strategies that can be tested *in vitro*, *in vivo*, and in clinical settings

[44]. Details of the network and the BD modeling scheme adopted and key findings for the cases reviewed in this section are summarized in Table 5.

Use of Trastuzumab or Herceptin, Pertuzumab and small-molecular inhibitor erlotinib drugs are well-known line of treatment for HER2-positive breast cancer specifically to block Erb2/Erb1 receptor induced deregulation of downstream signaling leading to tumor progression. BD modeling of a cancer cell line-specific signaling network constructed by constraining time-course proteomic data from three HER2-positive breast cancer cell-lines exposed to these drugs led to identification of specific new interactions that may strongly influence MAPK and PI3K activation patterns [142]. Specifically, in HCC1974, which is Trastuzumab resistant, the identified two new edges PDK1 → ErbB-2 and p70S6K→Akt introduced feedback loops resulting in suppression of apoptosis phenotype via PI3K pathway and thereby causing stabilization of Trastuzumab drug-resistance by promoting oncogenic effects. Observations in the clinical breast cancer samples substantiate these predictions [143]. Use of inhibitors such as celecoxib [144] against PDK1 could help overcome such a drug-resistance. Herceptin-based treatment targets the extracellular domain IV of HER2 which in turn down-regulates activation of MAPK pathways, *viz.*, specifically ERK1/2, p38, and JNK1/2, and thereby regulating signal flow toward mitogenic and survival phenotypes [145]. However, clinical data revealed that ~70% of the initial responders to Herceptin subsequently experienced progression to metastasis [146] suggesting the possibility of drug-resistance [147,148]. BD modeling of the underlying network showed that dynamic variations in the levels of several dual-specificity phosphatases (DUSPs), which too regulate MAPK pathways, could provide insights into targeting certain DUSP to overcome resistance against Herceptin drug treatment [149]. In fact, gene expression analysis on clinical samples from a HER2-positive cohort receiving Herceptin treatment shows that higher expression of DUSP4 may be correlated with poor patient survival [150] making it a potential target. Therefore, inhibiting DUSP4 expression could help overcome Herceptin drug-resistance. Probabilistic Boolean modeling of a breast cancer signaling network corroborated with siRNA gene silencing experiments on MDA-MB-435 cell line suggested that Mcl1 is a good drug target for influencing cancer cell growth [151].

Systematic attractor landscape analysis of 45 distinct cancer cell-specific p53 networks perturbed with small-molecular inhibitors predicted the phenotype switching affected [152]. Small-molecule inhibitors used include Nutlin-3 [153] for p53-MDM2 interaction, GSK2830371 [154] for Wip1, MK-2206 [155] for Akt, CDK2 inhibitors [156] for Cyclin E, and Navitoclax [157,158] for BCL2 family proteins along with or without DNA damaging drug

**TABLE 5** Novel therapeutic targets predicted by Boolean dynamic modeling of various networks based on cancer drug response and resistance. Construction objective adopted and the network statistics are specified. While S and GA refer respectively to synchronous and general asynchronous update methods described in section 2.1, PB refers to probabilistic Boolean modeling [166,167]

| Cancer type | Construction objective | Compartment | Nodes | Links | Update scheme | Therapeutic targets |
|---|---|---|---|---|---|---|
| Combination targets to circumvent drug resistance | | | | | | |
| Gastric cancer [173] | Knowledge-driven | Intracellular | 75 | 149 | GA | TAK1 with PI3K or AKT |
| Colon cancer [49] | Knowledge-driven | Intracellular and tumor microenvironment | 70 | 153 | GA | C2-ceramide with PI3K/AKT pathway |
| Breast cancer [151] | Knowledge-driven | Intracellular | 31 | 56 | PB | Mcl1 |
| Cancer drug response and resistance | | | | | | |
| Breast cancer [142] | Knowledge-driven | Intracellular | 11 | 26 | S | Edge between PDK1 and ErbB2 or p70S6K and Akt |
| Pan cancer [152] | Data-driven | Intracellular | 16 | 41 | S | AKT, BCL2, Cyclin E, Wip1, and p53-MDM2 with DNA |
| Colorectal cancer [165] | Knowledge-driven | Intracellular | 95 | 341 | PB | Feedback edge with Src |
| Breast cancer [170] | Knowledge-driven | Intracellular | 20 | 22 | GA | TNFα with JAK-STAT and PI3K-AKT |

etoposide. Networks used were constructed using genomics data from 83 human cancer cell-lines. Specifically, this study showed that single inhibition of Akt and combinations such as inhibition of p53-MDM2 and Wip1 with or without DNA-damaging drug may offer high efficacy. While Akt is a promising therapeutic target for overcoming cell-type-specific drug-resistance, given that it has multiple functional sites and is involved in several feedbacks [159], triple inhibition instead of single may be necessary [160].

A therapeutic drug inhibiting a target node can cause cells to offer adaptive resistance, wherein the inhibitor, such as that against RAS, may induce dynamic reprogramming of the signaling process to adapt to new treatment conditions [161–163]. In such cases, it is imperative to identify the aspects of the signaling network responsible for such dynamic reprogramming and arrest the same. For instance, employing novel probabilistic BD modeling on a colorectal cancer network showed that blocking a feedback regulation involving Src may overcome the adaptive resistance during targeted therapy involving inhibition of MAPK pathway [164,165]. Probabilistic BD modeling permits including variability in selecting the Boolean logic employed in the Boolean function of a node based on the weights of the interactions input it [166,167].

Emerging evidences suggest that interaction of cancer tissues with microenvironment consisting of inflammation-related cells such as macrophages may influence drug responses [168]. *In vitro* studies on MDA-MB-231 cell lines suggest that the efficacy of etanercept, a TNFα inhibitor may be compromised due to activation of other pathways triggered by macrophages-secreted cytokines and chemokines [169]. BD model of the TNFα signaling network integrated with JAK-STAT and PI3K-AKT pathways triggered by interleukins and other growth factors suggests that cells exposed to etanercept may continue to express survival phenotype due to NFκB activation triggered by these extracellular stimuli [170].

Systematic *in silico* analysis of perturbed BD model of colitis-associated colon cancer along with experimental validations revealed that concurrent activation of ceramide and inhibition of PI3K/AKT pathway could lead to an effective anti-cancer response in tumor cells [49]. Availability of several inhibitors [171] of PI3K/AKT pathway that are under clinical evaluation and of C2-ceramide that increases endogenous levels of ceramide [172] makes this combinatorial targeting attractive. Attractor analysis of a BD model of gastric adenocarcinoma cells suggested that besides the traditional combinatorial inhibitors such as that for PI3K and MEK, and for MEK and AKT currently investigated in clinical trials for different cancers, simultaneous targeting of TAK1 and PI3K, and of TAK1 and AKT could favor apoptotic phenotype [173].

Cancer tissue-specific BD models led to identification of the causes of poor efficacy of a treatment regime and the mechanism such as dynamic reprogramming

underlying acquired drug-resistance during a certain therapy. BD analysis further led to identification of potential combinatorial treatment targeting specific nodes or interactions that could circumvent emergence of drug-resistance.

# 6 | PERSPECTIVES

Ability to predict and understand causal mechanisms governing cancer incidence and progression is paramount to preventing, managing, and combating the disease. Cancer is widely recognized as a result of disturbance in the signaling problem due to aberrant cues, source for which could be external or internal to cells [2]. BD modeling approaches are used extensively to predict prognostic markers, to decipher mechanisms governing cancer progression and to identify novel therapeutic targets for improving disease management strategies. While these predictions offer novel insights, most of the BD models in literature (Tables 3–5) primarily consider intracellular signal flow, which accounts for only a small fraction of the tissue-level cancer signaling process. It is well recognized that tumor formation and cancer progression are orchestrated by complex dynamic communication between various inter- and intra-cellular machinery [2,174,175]. We present in Figure 3 a block diagram capturing dynamic communication that may be present between different cancer-related signaling machinery. The functioning of each of these machineries is in turn governed by interacting entities such as protein, mRNA, small molecules at multiple levels.

Unraveling etiology of tumor formation and its eventual dynamic responses require a cancer-specific model that incorporates the multi-cellular signaling process elucidated in Figure 3. Such a model will juxtapose signal flow within a cancerous cell and that in other cells in the tumor microenvironment, with detailed communication between them. This poses challenge at two-levels, *viz.*, constructing a reliable BD model of the comprehensive network and performing massive computations of the same.

A step towards addressing the first challenge could be constructing and analyzing cancer-specific BD model of each of the signaling machinery (in Figure 3) under isolated conditions. Subsequently validate the predictions using experimentally measured threshold levels of observable nodes and exhibited phenotypes. Key bottleneck here could be lack of knowledge of 1. entities and interactions participating in the considered machinery and 2. which sub-machineries may further be involved. Should a network under normal conditions be available, the first bottleneck could be circumvented by identifying the perturbations in the nodes or interactions or associated
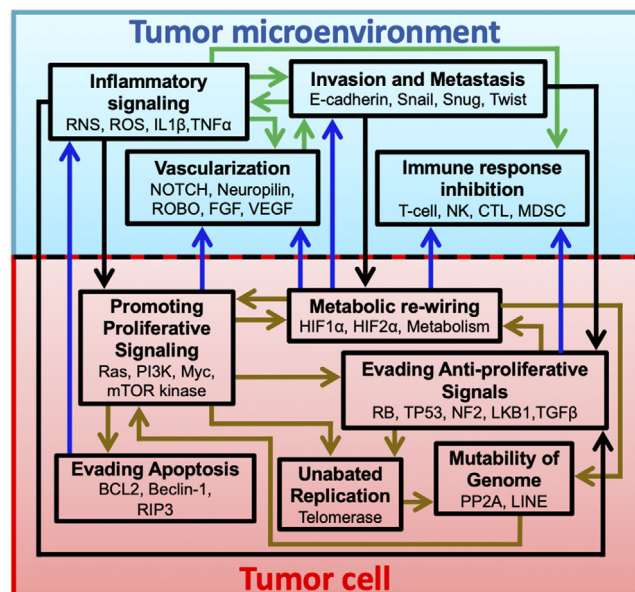


**FIGURE 3** Block diagram of different signaling machinery (boxes) influencing cancer incidence, orchestration and progression along with a few important entities in it. Signaling machinery in the lower (red) and upper (cyan) sections, respectively, correspond to the cases wherein signal transduction occurs within a tumor cell and in its microenvironment. Communication between signaling machinery within tumor cells and between those in its microenvironment are captured respectively by golden and green arrows. Blue arrows represent paracrine communication between tumor cells and its microenvironment, and vice-versa is captured by black ones

Boolean logic or a combination thereof that may predict a certain observed phenotype. However, addressing the second bottleneck is harder. For example, consider the case of cancer progression machinery such as "Invasion and Metastasis" (Figure 3). While involvement of several intracellular entities such as Snail in this machinery is well-known [112], emerging evidences suggest that mechanotransduction – signal flow triggered by mechanical cues from local microenvironment – can modulate the signaling process [176–181]. Further, recent studies show that pro-survival autophagy machinery induced by shear [182,183] may govern the key short timescale processes such as intravasation and extravasation during metastasis, seeding of which could be by polyclonal cell clusters [184]. Detailed mechanisms that regulate mechanotransduction are as yet unavailable and has attracted attention only in the recent years [177,181], which calls for improving knowledgebase on these aspects. Moreover, it is unclear how mechanical cue dynamics involving diffusion of species in physical dimensions can be incorporated in BD modeling framework, which requires variables to be strictly discrete. Combining agent-based modeling approach which permits capturing such tumor microenvironment

dynamics along with the BD model of intracellular signaling could address this limitation of discrete dynamic modeling approaches [185].

Well-benchmarked individual machinery models could then be used in a plug-and-play mode to create a comprehensive, integrated BD model. Such a model should incorporate intracellular signal transduction and other processes occurring in the tumor microenvironment, and more importantly communication between them (Figure 3). Use of ROA update method further permits incorporation of heterogeneity in both inter- and intracellular interactions [186,187]. This can enable incorporating ensemble-level features such as seeding metastasis by tumor cell clusters [184], cell-to-cell abundance variability. Heterogeneity is capitalized by cancer cells for various purposes such as relapse [127,188]. Such integrated models can be used for 1. precisely predicting the dynamic orchestration of attractors representing tumor formation, growth and progression and the associated critical nodes or interactions within and outside a cancer cell, 2. deciphering dynamic reprogramming of normal long- and short-range biological processes such as metabolism within tumor cell [10–15], EMP [110,111] and 3. identifying, from the critical orchestrators and those regulating them, with significant confidence, potential candidates that enable phenotype switching for targeted therapies.

Emerging novel therapeutic strategies range from using microorganisms such as bacteria [189,190], nanoparticles [191] as carriers for delivery of drugs deep inside tumors to using genome editing technology for different cancers [192] to reprogramming metabolic pathways [193]. Since delivery agents or metabolic reprogramming could exhibit deleterious influence or undesired outcomes on the host normal or cancer cells, an integrated model can help unravel their short- and long-range (side-) effects, presence of inherent resistance to drugs or even drug-resistance induced by them. These are paramount to effective drug administration and disease management. Further, a comprehensive BD model trained with multiscale measurements [194] such as proteomics, genomics, RNAseq at scales ranging from single-cell to whole-body levels for identifying attractor phenotypic patterns can reflect the physiological state of an individual [195,196]. An omics data-tuned patient-specific model can provide insights into designing personalized therapy and novel disease management strategies [35,196–199].

While a BD model consisting of large number of interacting nodes along with associated Boolean logic can be assembled, capitalizing it for useful purposes requires finding the one-step state transition matrix ($T$). Estimation of $T$ is a computationally tedious task, especially when random order asynchronous update method is employed. Reasons for this are three-fold: 1. finding all possible FP, cyclic, and complex attractors, 2. computing large number of states needed for constructing reasonably sized STG, 3. computing frequency of permutations corresponding to every pair of states in the STG. While efficient algorithms are becoming available for finding primary attractors in large-scale Boolean networks [98], development of an effective tool for estimating $T$ is needed. We posit that this tool will strongly hinge on the ability to identify the smallest size of the STG that preserves all the necessary characteristics. We further believe use of AI-based methods could address these challenges effectively. While most BD models of cancer network consider use of FP attractors, a question arises as to what are the practical implications of cyclic attractors, if any found and how its features can be harnessed for useful purposes.

BD modeling predictions are based on qualitative relationships between the entities in the network, and thus information pertaining to subtle underlying dynamics is sacrificed. For instance, BD models fail to predict precise bifurcation or switch-like behavior dictated by the actual kinetics and associated parameters governing signal flow. This is a well-recognized severe limitation of discrete dynamic models. Using multi-valued logical variables, which increases computational complexities pertaining to evaluation of the Boolean functions, or fuzzy logic instead of Boolean logic [33,200] could address this limitation to some extent [31,48]. However, it can at best capture these subtle behaviors as state-change patterns only [201]. As discussed earlier, BD models currently cannot account for certain continuous processes such as diffusion in physical dimensions. Diffusion of various species is an important contributor in communication between a tumor cell and its microenvironment. Capturing these factors is necessary from a holistic perspective. Development of new tools that can account for these cancer-related factors while efficiently estimating $T$ is needed to build a large predictive cancer-specific BD model. A recently proposed novel approach to combine BD modeling and agent-based framework via PhysiBoSS tool [185] accounting for diffusion of species in tumor microenvironment is a small, promising step in this direction.

## AUTHOR CONTRIBUTIONS
Data curation, funding acquisition, investigation, methodology, resources, software, validation, visualization,

writing-review and editing: Shubhank Sherekar and Ganesh A. Viswanathan.

## ORCID

*Ganesh A. Viswanathan* https://orcid.org/0000-0001-6424-0765

## REFERENCES

1. D. Hanahan and R. A. Weinberg, *The hallmarks of cancer*, Cell **100** (2000), 57–70.
2. D. Hanahan and R. A. Weinberg, *Hallmarks of cancer: The next generation*, Cell **144** (2011), 646–674.
3. Y. A. Fouad and C. Aanei, *Revisiting the hallmarks of cancer*, Am J Cancer Res. **7** (2017), 1016–1036.
4. J. Lopez and S. W. G. Tait, *Mitochondrial apoptosis: Killing cancer using the enemy within*, Brit J of Cancer **112** (2015), 957–962.
5. H. Sung, *Global cancer statistics 2020: GLOBOCAN estimates of incidence and mortality worldwide for 36 cancers in 185 countries*, CA Cancer J. Clin. **0** (2021), 1–41.
6. IARC. *GLOBOCAN 2020: New global cancer data*, 2020, March 18, 2021, available at https://gco.iarc.fr.
7. C.P. Wild, E. Weiderpass, and B.W. Stewart, (eds). *World cancer report: Cancer research for cancer prevention*, International Agency for Research on Cancer, Lyon, France, 2020.
8. Seventieth World Health Assembly, *Resolution WHA70.12. Cancer prevention and control in the context of an integrated approach*, World Health Organization, Geneva, Switzerland, 2017.
9. R. A. Weinberg, *Coming full circle - From endless complexity to simplicity and back again*, Cell **157** (2014), 267–271.
10. N. N. Pavlova and C. B. Thompson, *The emerging hallmarks of cancer metabolism*, Cell Metab. **23** (2016), 27–47.
11. R. A. Cairns, I. S. Harris, and T. W. Mak, *Regulation of cancer cell metabolism*, Nat. Rev. Cancer **11** (2011), 85–95.
12. R. A. Cairns and T. W. Mak, *The current state of cancer metabolism*, Nat. Rev. Cancer **16** (2016), 613–614.
13. R. J. DeBerardinis and N. S. Chandel, *Fundamentals of cancer metabolism*, Sci. Adv. **2** (2016), e1600200.
14. B. J. Altman, Z. E. Stine, and C. V. Dang, *From Krebs to clinic: glutamine metabolism to cancer therapy*, Nat. Rev. Cancer **16** (2016), 619–634.
15. C. S. Nanda, *Defining a metabolic landscape of tumors: genome meets metabolism*, Brit J of Cancer **122** (2020), 136–149.
16. P. Juin, *Decoding and unlocking the BCL-2 dependency of cancer cells*, Nat. Rev. Cancer **13** (2013), 455–465.
17. J. L. Koff, S. Ramachandiran, and L. Bernal-Mizrachi, *A time to kill: Targeting apoptosis in cancer*, Int. J. Mol. Sci. **16** (2015), 2942–2955.
18. V. Labi, M. Erlacher, *How cell death shapes cancer*, Cell Death. Dis. **6** (2015), e1675–e1675.
19. M. Kist, D. Vucic, *Cell death pathways: intricate connection and disease implications*, EMBO J. **40** (2021), e106700.
20. J. Luo, N. L. Solimini, and S. Elledge, *Principles of cancer therapy: Oncogene and non-oncogene addition*, Cell **136** (2009), 823–837.
21. B. Alberts, *The molecular biology of the Cell*, 6th ed., Garland Science, New York, NY, 2015.
22. Y. Lazebnik, *What are the hallmarks of cancer?*, Nat. Rev. Cancer **10** (2010), 232–233.
23. L. Pecorino, *Molecular biology of cancer: Mechanism, targets and therapeutics*, 2nd ed., Oxford Univ Press, Oxford, 2008.
24. D. J. L. Wong and A. Ribas, *Targeted therapy for melanoma*, Cancer Treat. Res. **167** (2016), 251–262.
25. M. K. Mayakar and T. G. Bivona, *Current landscape of targeted therapy in lung cancer*, Clin. Pharmacol. Ther. **107** (2017), 757–764.
26. V. Masoud and G. Pagès, *Targeted therapies in breast cancer: New challenges to fight against resistance*, World J. Clin Oncol **8** (2017), 120–134.
27. G. T. J. Zanudo, M. Scaltriti, and R. Albert, *A network modelling approach to elucidate drug resistance mechanisms and predict combinatorial drug treatments in breast cancer*, Cancer Converg. **1** (2017), 5.
28. A. C. Ventura, T. L. Jackson, and S. D. Merajver, *On the role of cell signalling models in cancer research*, Cancer Res. **69** (2009), 400–402.
29. U. Alon, *An introduction to systems biology: Design principles of biological circuits*, 2nd ed., CRC press, London, 2019.
30. G. Karlebach and R. Shamir, *Modeling and analysis of gene regulatory networks*, Nat. Rev. Mol. Cell Biol. **9** (2008), 770–780.
31. M. K. Morris, *Logic-based models for analysis of cell signalling networks*, Biochemistry **49** (2010), 3216–3224.
32. T. M. K. Cheng, *Understanding cancer mechanisms through network dynamics*, Briefings Funct. Genomics **6** (2012), 543–560.
33. W. Abou-Jaoude, *Logical modelling and dynamic analysis of cellular networks*, Front Genet. **7** (2016), 94.
34. R. Barbuti, *A survey of gene regulatory networks modelling methods: from diferential equations, to Boolean and qualitative bioinspired models*, J. Membr. Comput. **2** (2020), 207–226.
35. J. G. T. Zanudo, S. T. G. Steinway, and R. Albert, *Discrete dynamic network modelling of oncogenic signalling: Mechanistic insights for personalized treatment of cancer*, Curr. Opin. Syst. Biol. **9** (2018), 1–10.
36. S. Kauffman, *Metabolic stability and epigenesis in randomly constructed genetic nets*, J. Theor. Biol. **22** (1969), 437–467.
37. F. Li, *The yeast cell-cycle network is robustly designed*. Proc. Natl. Acad. Sci. USA **101** (2004), 4781–4786.
38. L. Mendoza, *A network model for the control of the differentiation process in Th cells*, Biosystems **84** (2006), 101–114.
39. A. Naldi, *Diversity and plasticity of Th cell types predicted from regulatory network modelling*, PLoS Comput. Biol. **6** (2010), e1000912.
40. S. A. Kauffman, *The origins of order: Self-organization and selection in evolution*, Oxford University Press, New York, 1993.
41. M. Cereda, T. P. Mourikis, and F. D. Ciccarelli, *Genetic redundancy, functional compensation, and cancer vulnerability*, Trends Cancer **2** (2016), 160–162.
42. R. Somogyi and C. A. Sniegoski, *Modeling the complexity of genetic networks: Understanding multigenic and pleiotropic regulation*, Complexity **1** (1996), 45–63.
43. A. Saadatpour, I. Albert, and R. Albert, *Attractor analysis of asynchronous Boolean models of signal transduction networks*, J. Theor. Biol. **266** (2010), 641–656.
44. J. D. Schwab, *Concepts in Boolean network modelling: What do they all mean?*, Comp. Struct. Biotech. J. **18** (2020), 571–582.

45. A. Saadatpour, *Dynamical and structural analysis of a T-cell survival network identifies novel candidate therapeutic targets for large granular lymphocyte leukemia*, PLoS Comput. Biol. **7** (2011), e1002267.

46. R. Albert and H. G. Othmer, *The topology of the regulatory interactions predicts the expression pattern of the segment polarity genes in Drosophila melanogaster*, J. Theor. Biol. **223** (2003), 1–18.

47. R. Zhang, *Network model of survival signaling in large granular lymphocyte leukemia*, Proc. Natl. Acad. Sci. USA **105** (2008), 16308–16313.

48. R. Schlatter, *ON/OFF and beyond - A boolean model of apoptosis*, PloS Comp. Biol. **5** (2009), e1000595.

49. J. Lu, *Network modelling reveals the mechanism underlying colitis-associated colon cancer and identifies novel combinatorial anti-cancer targets*, Sci. Rep. **5** (2015), 14739.

50. V. Balbas-Martinez, *A systems pharmacology model for inflammatory bowel disease*, PLoS One **13** (2018), 1–19.

51. B. He and K. Tan, *Understanding transcriptional regulatory networks using computational models*, Curr. Opin. Genet. Dev. **37** (2016), 101–108.

52. Y. Chen, *Core transcriptional regulatory circuitries in cancer*, Oncogene **39** (2020), 6633–6646.

53. Y. Xin, B. Cummins, and T. Gedeon, *Multistability in the epithelial-mesenchymal transition network*, BMC Bioinf. **21** (2020), 71.

54. J. P. Thiery and J. P. Sleeman, *Complex networks orchestrate epithelial-mesenchymal transitions*, Mol. Cell. Biol. **7** (2006), 131–142.

55. S. Klemm and S. Bornholdt, *Stable and unstable attractors in Boolean networks*, Phys. Rev. **72** (2005), 1–4.

56. A. Fauré, *Dynamical analysis of a generic Boolean model for the control of the mammalian cell cycle*, Bioinf. **22** (2006), 124–131.

57. A. Garg, *Synchronous versus asynchronous modeling of gene regulatory networks*, Bioinf. **24** (2008), 1917–1925.

58. M. Hopfensitz, *Attractors in Boolean networks : A tutorial*, Comput. Stat. **28** (2012), 19–36.

59. A. Saadatpour and R. Albert, *Boolean modeling of biological regulatory networks: A methodology tutorial*, Methods **62** (2013), 3–12.

60. M. Chaves, R. Albert, and E. D. Sontag, *Robustness and fragility of Boolean models for genetic regulatory networks*, J. Theor. Biol. **235** (2005), 431–49.

61. E. K. O'Shea and J. M. Raser, *Noise in gene expression: Origins, consequences, and control*, Science **309** (2005), 2010–2013.

62. A. Raj and A. Van Oudenaardan, *Nature, nurture, or chance: Stochastic gene expression and its consequences*, Cell **135** (2008), 216–226.

63. CoLoMoTo, *The CoLoMoTo consortium*, December 28, 2020, available at http://www.colomoto.org.

64. S. Kim, *Can Markov chain models mimic biological regulation?*, J. Biol. Sci. **10** (2002), 337–357.

65. J. A. Papin, T. Hunter, B.O. Palsson, S. Subramaniam, *Reconstruction of cellular signalling networks and analysis of their properties*, Nat. Rev. Mol. Cell Biol. **6** (2005), 99–111.

66. G. A. Viswanathan, *Getting started in biological pathway construction and analysis*, PLoS Comput. Biol. **4** (2008), e16.

67. D. Türei, T. Korcsmáros, and J. Saez-Rodriguez, *OmniPath: Guidelines and gateway for literature-curated signaling pathway resources*, Nat. methods **13** (2016), 966–967.

68. A. Subramanian, *A next generation connectivity map: L1000 platform and the first 1,000,000 profiles*, Cell **171** (2017), 1437–1452.

69. I. Papatheodorou, *Expression atlas update: From tissues to single cells*, Nucleic. Acids. Res. **48** (2020), D77–D83

70. Y. Li, *Expansion of biological pathways based on evolutionary inference*, Cell **158** (2014), 213–225.

71. T. Li, *GeNets: A unified web platform for network-based genomic analyses*, Nat. Methods **15** (2018), 543–546.

72. D. Szklarczyk, *STRINGv10: Protein–protein interaction networks, integrated over the tree of life*, Nucleic. Acids. Res. **43** (2015), D447–D452.

73. T. Li, *A scored human protein–protein interaction network to catalyze genomic interpretation*, Nat. Methods **14** (2017), 61–64.

74. G. Joshi-Tope, *Reactome: A knowledgebase of biological pathways*, Nucleic. Acids. Res. **33** (2005), D428–D438.

75. A. Krämer, *Causal analysis approaches in ingenuity pathway analysis*, Bioinf. **30** (2014), 523–530.

76. S. Choobdar, *Assessment of network module identification across complex diseases*, Nat. Methods **16** (2019), 843–852.

77. B. Luo, H.W. Cheung, A. Subramanian, and T. Sharifnia, *Highly parallel identification of essential genes in cancer cells*, Proc. Natl. Acad. Sci. USA **105** (2008), 20380–20385.

78. H. W. Cheung, *Systematic investigation of genetic vulnerabilities across cancer cell lines reveals lineage-specific dependencies in ovarian cancer*, Proc. Natl. Acad. Sci. USA **108** (2011), 12372–12377.

79. R. Marcotte, *Essential gene profiles in breast, pancreatic, and ovarian cancer cells*, Cancer Discov. **2** (2012), 172–189.

80. G. S. Cowley, *Parallel genome-scale loss of function screens in 216 cancer cell lines for the identification of context-specific genetic dependencies*, Sci. Data **1** (2014), 1–12.

81. A. Tsherniak, *Defining a cancer dependency map*, Cell **170** (2017), 564–576.

82. J. Barretina, *The Cancer Cell Line Encyclopedia enables predictive modelling of anticancer drug sensitivity*, Nature **483** (2012), 603–607.

83. CellDesigner.org, *CellDesigner^{TM}: A modeling tool of biochemical networks*, December 29, 2020, available at http://www.celldesigner.org.

84. Cytoscape. *Cytoscape. Network data integration, analysis, and visualization in a box*, December 29, 2020, available at http://www.cytoscape.org.

85. M. Hucka, *The systems biology markup language (SBML): Language specification for level 3 version 2 core release 2*, J. Integr. Bioinform. **16** (2019), 20190021.

86. F. M. Khan, *Unraveling a tumor type-specific regulatory core underlying E2F1-mediated epithelial mesenchymal transition to predict receptor protein signatures*, Nat. Commun. **8** (2017), 1–15.

87. S. Bilke and F. Sjunnesson, *Stability of the kauffman model*, Phys. Rev. E **65** (2001), 016129.

88. A. Veliz-Cuba, *Steady state analysis of Boolean molecular network models via model reduction and computational algebra*, BMC Bioinf. **15** (2014), 221.

89. R. S. Wang, A. Saadatpour, and R. Albert, *Boolean modeling in systems biology: an overview of methodology and applications*, Phys. Biol. **9** (2012), 055001.

90. J. Iovanna, *Implementing biological markers as a tool to guide clinical care of patients with pancreatic cancer*, Transl. Oncol. **14** (2021), 100965.

91. L. A. Garraway, J. Verweij, and K. V. Ballman, *Precision oncology: An overview*, J. Clin. Oncol. **31** (2013), 1803–1805.

92. B. Vogelstein, *Cancer genome landscapes*, Science **339** (2013), 1546–1558.

93. K. H. Allison and G. W. Sledge, *Heterogeneity and cancer*, Oncology **28** (2014), 772–778.

94. L. M. Coussens, L. Zitvogel, and A. K. Palucka, *Neutralizing tumor-promoting chronic inflammation: a magic bullet?*, Science **339** (2013), 286–291.

95. A. Mantovani, *Cancer-related inflammation*, Nature **454** (2008), 436–444.

96. E. Bonavita, *Antoagonistic inflammatory phenotypes dictate tumor fate and responses to immune checkpoint blockade*, Immunity **53** (2020), 1215–1229.

97. Z. Mai, H. Liu, *Boolean network-based analysis of the apoptosis network: Irreversible apoptosis and stable surviving*, J. Theor. Biol. **259** (2009), 760–769.

98. S. M. Choo and K. H. Cho, *An efficient algorithm for identifying primary phenotype attractors of a large-scale Boolean network*, BMC Sys. Biol. **10** (2016), 95.

99. R. M. Locksley, N. Killeen, and M. J. Lenardo, *The TNF and TNF receptor superfamilies: Integrating mammalian biology*, Cell **104** (2001), 487–501.

100. B. B. Aggarwal, S. C. Gupta, and J. H. Kim, *Historical perspectives on tumor necrosis factor and its superfamily: 25 years later, a golden journey*, Blood **119** (2011), 651–665.

101. S. L. Spencer, *Non-genetic origins of cell-to-cell variability in TRAIL induced apoptosis*, Nature **459** (2009), 428–432.

102. L. Calzone, *Mathematical modelling of cell-fate decision in response to death receptor engagement*, PLoS Comp. Biol. **6** (2010), e1000702

103. S. Vasaikar, *HSP70 mediates survival in apoptotic cells—Boolean network prediction and experimental validation*, Front Cell Neurosci **9** (2015), 1–12.

104. H. F. Fumia and M. L. Martins, *Boolean network model for cancer pathways predicting carcinogenesis and targeted therapy outcomes*, PLoS One **8** (2013), e69008.

105. T. Santarius, *A census of amplified and overexpressed human cancer genes*, Nat. Rev. Cancer **10** (2010), 59–64.

106. C. Biane and F. Delaplace, *Causal reasoning on boolean control networks based on abduction: Theory and application to cancer drug discovery*, IEEE/ACM Trans. Comput. Biol. Bioinf. **16** (2019), 1574–1585.

107. V. V. Rossato, *Towards the contribution of the p38 MAPK pathway to the dual role of TGFβ in cancer: A Boolean model approach*, Comp. Biol. Med. **104** (2019), 235–240.

108. L. Adlung, *Protein abundance of AKT and ERK pathway components governs cell type-specific regulation of proliferation*, Mol. Sys. Biol. **13** (2017), 904.

109. L. Grieco, *Integrative modelling of the influence of the MAPK network on cancer cell fate decision*, PLoS Comp. Biol. **9** (2013), e1003276.

110. C. L. Chaffer and R. A. Weinberg, *A perspective on cancer cell metastasis*, Science **331** (2011), 1559–1564.

111. N. Ma and S. S. Jeffrey, *Deciphering cancer clues from blood*, Science **367** (2020), 1424–1425.

112. J. S. Wu, *Plasticity of cancer cell invasion: Patterns and mechanisms*, Transl. Oncol. **14** (2021), 100899.

113. E. D. Williams, *Controversies around epithelial-mesenchymal plasticity in cancer metastasis*, Nat. Rev. Cancer **19** (2019), 719.

114. M. K. Jolly, *Implications of the hybrid epithelial/mesenchymal phenotype in metastasis*, Front. Oncol. **5** (2015), 155.

115. M. K. Jolly, *Stability of the hybrid epithelial/mesenchymal phenotype*, Oncotarget **7** (2016), 27067–27084.

116. M. A. Nieto, *EMT: 2016*, Cell **166** (2016), 21–45.

117. P. B. Gupta, *Phenotypic plasticity: Driver of cancer initiation, progression, and therapy resistance*, Cell Stem Cell **24** (2019), 65–78.

118. J. J. Bravo-Cordero, L. Hodgson, and J. Condeelis, *Directed cell invasion and migration during metastasis*, Curr. Opin. Cell Biol. **24** (2012), 277–283.

119. N. Reymond, B. B. D'Agua, and A. J. Ridley, *Crossing the endothelial barrier during metastasis*, Nat. Rev. Cancer **13** (2013), 858–870.

120. S. N. Steinway, *Network modelling of TGFb signalling in hepatocellular carcinoma epithelial-to-mesenchymal transition reveals joint Sonic hedgehog and Wnt pathway activation*, Cancer Res. **74** (2014), 5963–5977.

121. H. Yamamoto, *Wnt5a signalling is involved in the aggressiveness of prostate cancer and expression of metalloproteinase*, Oncogene **29** (2020), 2036–2046.

122. D. M. Nanus and P. Giannakakou, *Cancer therapies that are gone with the Wnt*, Science **349** (2015), 1283–1284.

123. D. T. Miyamoto, *RNA-Seq of single prostate CTCs implicates noncanonical Wnt signalling in antiandrogen resistance*, Science **349** (2015), 1351–1356.

124. S. N. Steinway, *Combinatorial interventions inhibit TGFβ-driven epithelial-to-mesenchymal transition and support hybrid cellular phenotypes*, NPJ Sys. Biol. Appl. **1** (2015), 1–12.

125. D. P. A. Cohen, *Mathematical modelling of molecular pathways enabling tumor cell invasion and migration*, PLoS Comp. Biol. **11** (2015), e1004571.

126. M. Chanrion, *Concomitant Notch activation and p53 deletion trigger epithelial-to-mesenchymal transition and metastasis in mouse gut*, Nat. Commun. **5** (2014), 1–5.

127. A. F. Gazdar, *Morphologic and other forms of heterogeneity in small cell lung cancer. What can we learn from them?*, J. Thora. Oncol. **13** (2018), 148–150.

128. Clinical Lung Cancer Genome Project (CLCGP), Network Genomic Medicine (NGM), *A genomic-based classification of human lung tumors*, Sci. Transl. Med. **5** (2013), 209ra153.

129. A. R. Udyavar, *A transcription factor network model explains heterogeneity and reveals a novel hybrid phenotype in small-cell lung cancer*, Cancer Res. **77** (2017), 1063–1074.

130. M. Yu, *Circulating breast tumor cells exhibit dynamic changes in epithelial and mesenchymal composition*, Science **339** (2013), 580–584.

131. M. Lu, *MicroRNA-based regulation of epithelial-hybrid-mesenchymal fate determination*, Proc. Natl. Acad. Sci. USA **110** (2013), 18144–18149.

132. J. Zhang, *TGF-beta-induced epithelial-to-mesenchymal transition proceeds through stepwise activation of multiple feedback loops*, Sci. Signal **7** (2014), ra91–ra91.

133. A. Grosse-Wilde, *Stemness of the hybrid epithelial/mesenchymal state in breast cancer and its association with poor survival*, PLoS One **10** (2015), e0126522.

134. J. I. Joo, J. X. Zhou, S. Huang, K.H. Cho, *Determining relative dynamic stability of cell states using Boolean network model*, Sci. Rep. **8** (2018), 1–4.

135. J. X. Zhou, *Relative stability of network states in Boolean network models of gene regulation in development*, Biosystems **142** (2016), 15–24.

136. K. Hari, *Identifying inhibitors of epithelial-mesenchymal plasticity using a network topology-based approach*, NPJ Sys. Biol. Appl. **6** (2020), 1–2.

137. F. Font-Clos, S. Zapperi, and C.A. LaPorta, *Topography of epithelial-mesenchymal plasticity*, Proc. Natl. Acad. Sci. **115** (2018), 5902–5907.

138. National Cancer Institute, *Drugs approved for different types of cancer*, December 29, 2020, available at https://www.cancer.gov/about-cancer/treatment/drugs/cancer-type.

139. A. Li and R.C. Bergen, *Clinical trial design: Fast, present and future in the context of bigdata and precision medicine*, Cancer **126** (2020), 4838–4846.

140. T. J. Lynch, *Activating mutations in the epidermal growth factor receptor underlying responsiveness of non–small-cell lung cancer to gefitinib*, N. Engl. J. Med. **350** (2004), 2129–2139.

141. M. Maemondo, *Gefitinib or chemotherapy for non-small-cell lung cancer with mutated EGFR*, N. Engl. J. Med. **362** (2010), 2380–2388.

142. S. Von der Heyde, *Boolean ErbB network reconstructions and perturbation simulations reveal individual drug response in different breast cancer cell lines*, BMC Syst. Biol. **8** (2014), 75.

143. M. Maurer, *3- phosphoinositide–dependent kinase 1 potentiates upstream lesions on the phosphatidylinositol 3-kinase pathway in breast carcinoma*, Cancer Res. **69** (2009), 6299–6306.

144. P. H. Tseng, *Overcoming trastuzumab resistance in HER2-overexpressing breast cancer cells by using a novel celecoxib-derived phosphoinositide-dependent kinase-1 inhibitor*, Mol. Pharmacol. **70** (2006), 1534–1541.

145. T. Vu and F. X. Claret, *Trastuzumab: Updated mechanisms of action and resistance in breast cancer*, Front. Oncol. **2** (2012), 62.

146. D. Gajria and S. Chandarlapaty, *HER2-amplified breast cancer: Mechanisms of trastuzumab resistance and novel targeted therapies*, Expert Rev. Anticancer Ther. **11** (2011), 263–75.

147. K. L. Blackwell, *Single-agent lapatinib for HER2-overexpressing advanced or metastatic breast cancer that progressed on first- or second-line trastuzumab-containing regimens*, Ann. Oncol. **20** (2009), 1026–31.

148. Y. C. Wang, *Different mechanisms for resistance to trastuzumab versus lapatinib in HER2- positive breast cancers – role of estrogen receptor and HER2 reactivation*, Breast Cancer Res. **13** (2011), R121.

149. P. Buiga, *Regulation of dual specificity phosphatases in breast cancer during initial treatment with Herceptin: A Boolean model analysis*, BMC Syst. Biol. **12** (2018), 11.

150. O. Menyhart, *DUSP4 is associated with increased resistance against anti-HER2 therapy in breast cancer*, Oncotarget **8** (2017), 77207–77218.

151. P. Zhu, *Identification of potential drug targets in cancer signalling pathways using stochastic logical models*, Sci. Rep. **6** (2016), 23078.

152. M. Choi, *Network dynamics-based cancer panel stratification for systemic prediction of anticancer drug response*, Nat. Comm. **8** (2017), 1940.

153. M. V. Poyurovsky, *The C terminus of p53 binds the N-terminal domain of MDM2*, Nat. Struct. Mol. Biol. **17** (2010), 982–989.

154. A. Sriraman, *Cooperation of Nutlin-3a and a Wip1 inhibitor to induce p53 activity*, Oncotarget **7** (2016), 31623–31638.

155. H. Hirai, *MK-2206, an allosteric Akt inhibitor, enhances antitumor efficacy by standard chemotherapeutic agents or molecular targeted drugs in vitro and in vivo*, Mol. Cancer Ther. **9** (2010), 1956–1967.

156. M. Kitagawa, *Butyrolactone I, a selective inhibitor of cdk2 and cdc2 kinase*, Oncogene **8** (1993), 2425–2432.

157. J. Shi, *Navitoclax (ABT-263) accelerates apoptosis during drug-induced mitotic arrest by antagonizing Bcl-xL*, Cancer Res. **71** (2011), 4518–4526.

158. L. T. Alexander, *Type II inhibitors targeting CDK2*, ACS Chem. Biol. **10** (2015), 2116–2125.

159. C. Sun and R. Bernards, *Feedback and redundancy in receptor tyrosine kinase signalling: Relevance to cancer therapies*, Trends Biochm. Sci. **39** (2014), 465–474.

160. G. M. Nitulescu, *Akt inhibitors in cancer treatment: The long journey from drug discovery to clinical use*, Int. J. Oncol. **48** (2016), 869–885.

161. J. S. Duncan, *Dynamic reprogramming of the kinome in response to targeted MEK inhibition in triple-negative breast cancer*, Cell, **149** (2012), 307–321.

162. P. Lito, N. Rosen, and D. B. Solit, *Tumor adaptation and resistance to RAF inhibitors*, Nat. Med. **19** (2013), 1401–9.

163. G. L. Johnson, *Molecular pathways: Adaptive kinome reprogramming in response to targeted inhibition of the BRAF-MEK-ERK pathway in cancer*, Clin. Cancer Res. **20** (2014), 2516–2522.

164. S. H. Cho, *Attractor landscape analysis of colorectal tumorigenesis and its reversion*, BMC System Biol. **10** (2016), 96.

165. S. M. Park, *Feedback analysis identifies a combination target for overcoming adaptive resistance to targeted cancer therapy*, Oncogene **39** (2020), 3803–3820.

166. I. Shmulevich, *Probabilistic Boolean networks: A rule-based uncertainty model for gene regulatory networks*, Bioinformatics **18** (2002), 261–274.

167. P. Trairatphisan, *A probabilistic Boolean network approach for the analysis of cancer-specific signalling: A case study of deregulated PDGF signalling in GIST*, PLoS One **11** (2016), e0156223.

168. V. S. Jones, *Cytokines in cancer drug resistance: Cues to new therapeutic strategies*, Biochim. Biophys. Acta. **1865** (2016), 255–265.

169. S. Madhusudan, *A phase II study of etanercept (Enbrel), a tumor necrosis factor α inhibitor in patients with metastatic breast cancer*, Clin. Cancer Res. **10** (2004), 6528–6534.

170. E. Shirmohammadi, *The efficacy of etanercept as anti-breast cancer treatment is attenuated by residing macrophages*, BMC Cancer **20** (2020), 836.

171. M. Martini, *PI3K/AKT signaling pathway and cancer: An updated review*, Ann. Med. **46** (2014), 372–383.

172. B. Ogretmen, *Biochemical mechanisms of the generation of endogenous long chain ceramide in response to exogenous short chain ceramide in the A549 human lung adenocarcinoma cell line. Role for endogenous ceramide in mediating the action of exogenous ceramide*, J. Biol. Chem. **277** (2002), 12960–12969.

173. Å. Flobak, *Discovery of drug synergies in gastric cancer cells predicted by logical modeling*, PLoS Comput. Biol. **11** (2015), e1004426.

174. S. I. Grivennikov, F. R. Greten, and M. Karin, *Immunity, inflammation, and cancer*, Cell **140** (2010), 883–899.

175. S. L. Floor, *Hallmarks of cancer: Of all cancer cells, all the time?*, Trends Mol. Med. **18** (2012), 509–515.

176. P. A. Janmey and R. T. Miller, *Mechanisms of mechanical signalling in development and disease*, J. Cell. Sci. **124** (2011), 9–18.

177. J. M. Northcott, *Feeling stress: The mechanics of cancer progression and aggression*, Front Cell Dev. Biol. **6** (2018), 17.

178. F. Kai, A. P. Drain, and V. M. Weaver, *The extracellular matrix modulates the metastatic journey*, Dev. Cell **49** (2019), 332–346.

179. E. Hannezo and C. P. Heisenberg, *Mechanochemical feedback loops in development and disease*, Cell **178** (2019), 12–25.

180. J. Das, S. Chakraborty, and T. K. Maiti, *Mechanical stress-induced autophagic response: A cancer-enabling characteristic?*, Semin. Cancer Biol. **66** (2020), 101–109.

181. Y. Zhang and Z. Li, *RNA Binding proteins: Linking mechanotransduction and tumor metastasis*, Cancer Lett. **496** (2021), 30–40.

182. J. Das, *Hemodynamic shear stress induces protective autophagy in HeLa cells through lipid raft-mediated mechanotransduction*, Clin. Exp. Metastasis **35** (2018), 135–148.

183. X. Wang, *Fluid shear stress promotes autophagy in hepatocellular carcinoma cells*, Int. J. Biol. Sci. **14** (2018), 1277–1290.

184. K. J. Cheung and A. J. Ewald, *A collective route to metastasis: Seeding by tumor cell clusters*, Science **352** (2016), 167–169.

185. G. Letort, *PhysiBoSS: A multi-scale agent-based modelling framework integrating physical dimension and cell signalling*, Bioinformatics **35** (2019), 1188–1196.

186. A. Yachie-Kinoshita, *Modeling signaling-dependent pluripotency with Boolean logic to predict cell fate transition*, Mol. Sys. Biol. **14** (2017), e7952

187. B. C. Ross, *Simulating heterogeneous populations using Boolean models*, BMC Sys. Biol. **12** (2018), 1–11

188. Q. Li, *Dynamics inside the cancer cell attractor reveal cell heterogeneity, limits of stability, and escape*, Proc. Natl Acad. Sci. **13** (2016), 2672–2677.

189. N. Mehta, *Baterial carriers for glioblastoma therapy*, Mol. Ther. Oncolytics. **4** (2017), 1–17.

190. D. V. Araujo, *Bugs as drugs: The role of microbiome in cancer focussing on immunotherapeutics*, Cancer Treat. Rev. **92** (2021), 102125.

191. S. Senapati, *Controlled drug delivery vehicles for cancer treatment and their performance*, Sig. Trans Targeted Ther. **3** (2018), 7.

192. H. Li, *Applications of genome editing technology in the targeted therapy of human diseases: mechanisms, advances and prospects*, Sig. Trans. Targeted Ther. **5** (2020), 1.

193. N. Hay, *Reprogramming glucose metabolism in cancer: can it be exploited for cancer therapy?*, Nature Rev. Cancer. **16** (2016), 635–649.

194. K. J. Karczewski and M. P. Snyder, *Integrative omics for health and disease*, Nat. Rev. Genet. **19** (2018), 299–310.

195. J. Béal, *Personalization of logical models with multi-omics data allows clinical stratification of patients*, Front Physiol. **9** (2019), 1965.

196. J. T. Yurkovich, *A systems approach to clinical oncology uses deep phenotyping to deliver personalized care*, Nat. Rev. Clin. Oncol. **17** (2020), 183–194.

197. V. Prasad, T. Fojo, and M. Brada, *Precision oncology: Origins, optimism, and potential*, Lancet Oncol. **17** (2016), e81–e86.

198. A. Letai, *Functional precision cancer medicine — moving beyond pure genomics*, Nat. Med. **23** (2017), 1028–1035.

199. J. Saez-rodriguez and N. Blüthgen, *Personalized signaling models for personalized treatments*, Mol. Sys. Biol. **16** (2020), e9042.

200. B. B. Aldridge, *Fuzzy logic analysis of kinase pathway crosstalk in TNF/EGF/insulin-induced signalling*, PLoS Comp. Biol. **5** (2009), e1000340.

201. M. Wu, X. Yang, and C. Chan, *A dynamic analysis of IRS-PKR signalling in liver cells. A discrete modelling approach*, PLoS One **4** (2009), e8040.